

Molecular Orbital Calculations on Penta Coordinated Ferric Dithiocarbamates Exhibiting Intermediate and Low Spin Ground States

P. Ganguli and K. M. Hasselbach *

Institut für Anorganische und Analytische Chemie, Johannes Gutenberg-Universität, Mainz

Z. Naturforsch. **34a**, 1500–1506 (1979); received November 7, 1979 **

SCCEHMO calculations show that the ground state in $[\text{Fe}(\text{dte})_2\text{X}]$, $\text{X} = \text{Cl}, \text{Br}, \text{I}$ and NCS , is $^4\text{A}_2: (x^2 - y^2)^2(xz)^1(yz)^1(z^2)^1(xy)^0$ and for $\text{X} = \text{NO}$ is $^2\text{A}_1: (xz)^2(yz)^2(x^2 - y^2)^2(z^2)^1(xy)^0$. The calculated quadrupole splittings of iron and iodine included the valence shell, overlap charge, and the ligand and lattice contributions to the EFG tensor at the nuclei. In addition, the electron densities at the iron nucleus are compared with the measured isomer shifts. The spin densities may be interpreted in terms of a π -delocalization. The results are discussed on the basis of the molecular orbital energy level schemes.

Introduction

Penta coordinated Ferric dithiocarbamates have been the subject of various investigations due to their interesting electronic structures [1–6]. The iron(III) complexes $[\text{Fe}(\text{dte})_2\text{X}]$, where $\text{dte} = \text{NN}'\text{-dialkyl-dithiocarbamate}$ and $\text{X} = \text{Cl}, \text{Br}, \text{I}, \text{NCS}$, exhibit the rare intermediate $^4\text{A}_2$ ($S = 3/2$) ground state [1], whereas the complex with $\text{X} = \text{NO}$ is in the low spin state $^2\text{A}_1$ ($S = 1/2$) [6]. One of the ground state properties that has been thoroughly investigated is the electric field gradient (EFG) which may be deduced by measuring the electric quadrupole splitting (ΔE_Q) in a Mössbauer experiment. Though from ligand field theory the quadrupole splitting for the $^4\text{A}_2$ ground state is expected to be zero, the measured values of ΔE_Q in $[\text{Fe}(\text{dte})_2\text{X}]$, $\text{X} = \text{Cl}, \text{Br}, \text{I}, \text{NCS}$, are rather large ($\Delta E_Q \approx 2.7 \text{ mm/sec}$) [2].

Controversies exist on the origin of the EFG in these systems. An earlier crystal field calculation has attributed the EFG to large lattice contributions arising from a tetragonal distortion [7], whereas a molecular orbital calculation, on $[\text{Fe}(\text{dte})_2\text{Cl}]$ showed that the EFG is primarily caused by covalency effects [8, 9]. To study:

- a) the effects of the axial ligand on the electronic structure,

- b) the nature of bonding,

- c) the origin of the EFG in these systems, self consistent charge extended Hückel [10] molecular orbital (SCCEHMO) calculations [11, 12] on the series $[\text{Fe}(\text{dte})_2\text{X}]$, $\text{X} = \text{Cl}, \text{Br}, \text{I}, \text{NCS}$, and NO were carried out. The results of the MO calculations are compared with the results of Mössbauer, magnetic anisotropy and NMR measurements.

Method

The SCCEHMO method has widely been used to investigate the electronic structure of transition metal complexes [8, 9, 13–16, 34]. The diagonal elements of the Hamilton matrix were approximated by [8, 14]:

$$H_{ii} = -\alpha_i - k \Delta\alpha_i q^A \quad (1)$$

where α_i is the valence orbital ionisation potential (VOIP), $\Delta\alpha_i$ is the change in α_i by one unit of charge, q^A is the charge on the atom to which the orbital i belongs, and k is an empirical parameter $0 \leq k \leq 1$. The off-diagonal elements H_{ij} were calculated using the Wolfsberg Helmholtz approximation

$$H_{ij} = C S_{ij} \frac{1}{2} (H_{ii} + H_{jj}) \quad (2)$$

where S_{ij} is the overlap integral and for the constant a value of $C = 2.5$ was chosen, to keep counterintuitive mixing [17] reasonably small.

To compare the results with those of DeVries et al. [8, 9], their parameters were used; the additional parameters for Br , I , and O were taken from literature [18, 19] and are listed in Table 1.

* To whom correspondence should be addressed.

** First version was received on June 16, 1979.

Reprint requests to Dr. K. M. Hasselbach, Institut für Anorganische und Analytische Chemie, Johannes Gutenberg-Universität, Joh.-Joachim-Becher-Weg 24, D-6500 Mainz.



Table 1. Slater type orbitals [18–20] and valence orbital ionisation potentials.

Atom	<i>n l</i>	Exponent	α [eV]	$\Delta\alpha$ [eV]
H	1s	1.0	13.595	12.84
C	2s	1.6083	20.78	32.16
	2p	1.5679	11.32	11.37
N	2s	1.9237	25.16	13.09
	2p	1.917	14.16	14.28
O	2s	2.275	22.525	9.7
	2p	2.275	11.94	9.7
S	3s	2.1223	22.525	9.7
	3p	1.8273	11.94	9.7
Cl	3s	2.3561	25.93	10.34
	3p	2.0387	13.82	10.34
Fe	4s	1.4	7.9	7.95
	4p	1.56	4.55	6.85
	3d*	5.35		
	3d**	2.200	8.7	11.33
Br	4s	2.60	21.0	10.0
	4p	2.257	12.3	10.0
I	5s	2.4	21.6	10.0
	5p	2.20	11.3	10.0

* The coefficients in the double zeta iron 3d functions are 0.5661.

** 0.5860 respectively.

The basis set consisted of the ns and np single exponent Slater type atomic orbitals (STOs) of the valence shells of the ligand atoms, and for iron a 3d double zeta function, the 4s and 4p STOs were taken [20].

Molecular Structure

The structure of the compounds determined by single crystal x-ray analysis [21–25] was used in the SCCEHMO calculations. The general features of the structure and the coordinate system chosen are shown in Figure 1. In order to keep the number of basis orbitals reasonably small, the alkyl groups *R*, *R'* were replaced by hydrogen atoms. This approximation is not too drastic since the electric

and magnetic properties do not change very much with changes in the alkyl groups in the dithiocarbamate ligand [1, 2, 26].

Electric Field Gradient

The electric quadrupole splitting ΔE_Q for the $3/2^+ \rightarrow 1/2^+$ nuclear γ -transition in ^{57}Fe is calculated by

$$E_Q = \frac{1}{2} e Q V_{zz} \sqrt{1 + \eta^2/3} \quad (3)$$

where $Q = 0.21$ b is the nuclear quadrupole moment of the excited state of ^{57}Fe ; V_{zz} is the *z* component of the EFG tensor and η is the asymmetry parameter.

The tensor operator \hat{V}_{ij} is just the sum of the one electron operators \hat{v}_{ij} where

$$\hat{v}_{ij} = (1 - \gamma(r)) q (3 \hat{r}_i \hat{r}_j - \hat{r}^2 \delta_{ij}) / \hat{r}^5, \quad (4)$$

i, j = *x, y, z*; $\gamma(r)$ represents the Sternheimer shielding factor and *q* is the charge at point *f*.

The expectation value of \hat{V}_{ij} can be decomposed into contributions originating from the valence shell electrons of the central atom and into contributions from point charges distributed within the molecule. The valence contributions may be calculated using the operator-equivalence [27] formalism

$$\hat{v}_{ij} = e \langle \| v_{ij} \| \rangle (1 - R_{nl}) \langle r^{-3} \rangle_{nl} \cdot \left[\frac{1}{2} (\hat{l}_i \hat{l}_j + \hat{l}_j \hat{l}_i) - \frac{l(l+1)}{3} \delta_{ij} \right] \quad (5)$$

where $\langle \| v_{ij} \| \rangle$ is the reduced matrix element which takes on the value 2/7 for d-, 6/5 for p- and zero for s-electrons. The values used for the Sternheimer shielding factors are $R_{3d} = R_{4p} = 0.32$, and for the radial expectation values of r^{-3} of the 3d and 4p orbitals of the iron atom they are $\langle r^{-3} \rangle_{3d} = 5.1 a_0^{-3}$, $\langle r^{-3} \rangle_{4p} = 1.7 a_0^{-3}$ [34]. The ligand contribution to the EFG tensor can be calculated using (4) as a point charge approximation with $\gamma(r) = \gamma(\infty) = -9.1$ [28] and *q* representing the charges on the ligand atoms, which are calculated from the diagonal elements of the first order charge density and bond order matrix.

The overlap charges q^{AB} are obtained from the off-diagonal elements. The EFG-tensor arising from the contributions of the overlap charges is also calculated using (4) with the calculated overlap charges q^{AB} situated at some point r_i^{AB} on the line

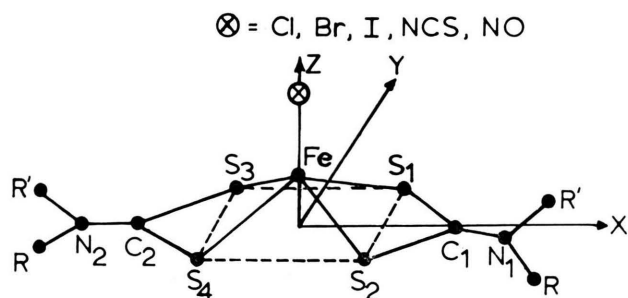


Fig. 1. Molecular structure of $[\text{Fe}(\text{dtc})_2\text{X}]$ and coordinate system.

connecting the two atoms A and B, where

$$r_i^{AB} = (1 - C_{AB}) r_i^A + C_{AB} r_i^B \quad (i = x, y, z). \quad (5)$$

C_{AB} was taken to be 1/2 when A and B were ligand atoms and was allowed to vary when A or B was iron. When the distance between the iron atom and a ligand atom is smaller than about 1.5 Å, the approximation $\gamma(r) = \gamma(\infty)$ is no longer valid [28] as $\gamma(r)$ varies from 0.32 to -9.1. As the accurate radial dependence of $\gamma(r)$ for Fe is not known, in the present calculation a value of $\gamma(r) = -9.1$ was taken. In order to compensate for the possibly too large value of $1 - \gamma(r)$, and as \hat{v}_{ij} is proportional to r^{-3} , C_{AB} in (9) is allowed to vary from 0.5 to 1.0, i.e. the overlap charge is located more towards the ligand atoms thereby reducing the overlap contributions to the EFG-tensor.

The lattice contributions to the EFG-tensor were calculated by taking the point charge contributions from about 2000 nearest neighbours into account where the charges on the atoms were taken from the MO calculations using a Mulliken charge distribution.

Results and Discussion

The energy level schemes based on the MO calculations are shown in Figure 2. The ground state in the case of $[\text{Fe}(\text{dtc})_2\text{X}]$, X = Cl, Br, I, NCS is 4A_2 : $(x^2 - y^2)^2(xz)^1(yz)^1(z^2)^1$. In all the cases the relatively high energy of the (xy) molecular orbital is responsible for the spin pairing of the fifth electron of the valence shell resulting in the intermediate 4A_2 ground state. This energy level scheme is in accordance with those proposed earlier by ligand field calculations [29]. The ordering of the orbital energies in case of $[\text{Fe}(\text{dtc})_2\text{NO}]$ has been subjected to much controversy. Gray, Bernal, and Billig [30] have found from their MO calculation $(xz)^2(yz)^2(x^2 - y^2)^2(xy)^1(z^2)^0$ whereas Goodman et al. [31], based on EPR experiments have suggested $(xy)^2(xz)^2(yz)^2(z^2)^1(x^2 - y^2)^0$, which agrees in so far with the energy level scheme for the nitrosyl complex found in the present calculation:

$$(xz)^2(yz)^2(x^2 - y^2)^2(z^2)^1(xz, \pi_x\text{NO})^0 \\ \cdot (yz, \pi_y\text{NO})^0(xy)^0$$

as the unpaired electron is in a (z^2) molecular orbital which is predominantly iron $3d_{z^2}$. This has also been suggested from IR [32], EPR [31], UV/vis [30],

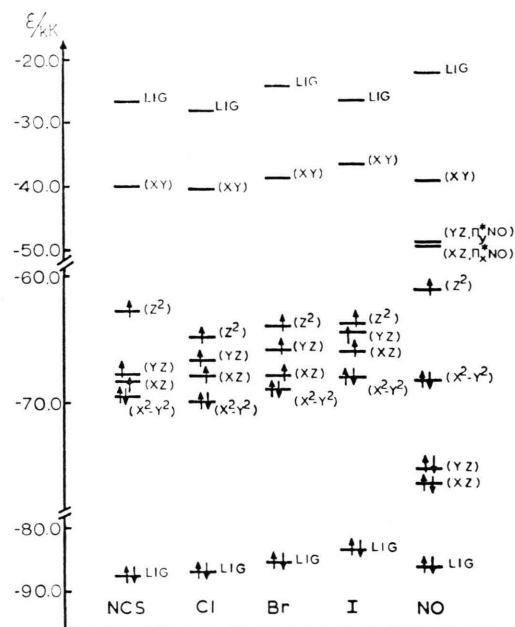


Fig. 2. Molecular energy level scheme for $[\text{Fe}(\text{dtc})_2\text{X}]$, X = NCS, Cl, Br, I, NO.

XPS [33], and kinetic studies on the nitrosyl complex. The $(xz, \pi_x\text{NO})$ and $(yz, \pi_y\text{NO})$ orbitals are lower in energy than the (xy) orbital due to the strong π -back donation of the NO group.

From symmetry considerations it is clear that $(x^2 - y^2)$ is essentially the nonbonding Fe ($3d_{x^2-y^2}$) orbital (coefficient 0.99); (xz) , (yz) are π -bonding and (z^2) is σ -bonding with respect to the axial ligand; (xy) is σ -bonding concerning the four sulphur atoms of the two dithiocarbamate ligands. As the (xy) , (xz) , (yz) , $(x^2 - y^2)$, (z^2) molecular orbitals consist mainly of the corresponding iron 3d atomic orbitals (coefficients ~ 0.9), to a first approximation the energy differences with respect to the non bonding $(x^2 - y^2)$ orbital, $\epsilon_{(z^2)} - \epsilon_{(x^2-y^2)}$ and $(\epsilon_{(xz)} + \epsilon_{(yz)})/2 - \epsilon_{(x^2-y^2)}$, would be a measure of the iron-axial ligand atom X σ - and π -interactions, respectively, as these splittings are expected to increase with increasing interaction. From Fig. 2 it then follows that for Fe-X the σ -interaction increases as X is $\text{I} < \text{Br} < \text{Cl} < \text{NCS} < \text{NO}$ and the π -interaction decreases as X is $\text{NO} > \text{I} > \text{Br} > \text{Cl} > \text{NCS}$. This ordering is also obvious from the coefficients of iron atomic orbitals in the occupied molecular orbitals. The fact that these compounds are highly covalent may be seen from the charges on the atoms listed in Table 2. All atoms remain

Table 2. Calculated charges on the atoms, electronic configuration of Fe and electron densities at the iron nucleus in $[\text{Fe}(\text{dtc})_2\text{X}]$.

$[\text{Fe}(\text{dtc})_2\text{X}]$ with X	Charges on the atoms					Electronic configuration of iron			Electron density ^b at the iron nucleus $ \Psi(0) ^2 a_0^{-3}$	Measured isomer shift ^c $\delta[\text{mm s}^{-1}]$
	Fe	X	S ^a	C ^a	N ^a	4s	4p	3d		
NCS	0.15450	S = − 0.44803 C = 0.36006 N = − 0.42965	− 0.05492	0.53532	− 0.57895	0.46	1.16	6.22	11 905 · 357	0.509 ± 0.008 ^d
Cl	0.16370	− 0.47149	− 0.15742	0.28714	− 0.22268	0.49	1.23	6.20	11 905 · 617	0.492 ± 0.008 ^d
Br	0.04489	− 0.39981	− 0.18540	0.29692	− 0.16229	0.51	1.23	6.20	11 905 · 549	0.492 ± 0.008 ^d
I	− 0.02844	− 0.28259	− 0.15875	0.27609	− 0.20956	0.51	1.26	6.26	11 905 · 411	0.509 ± 0.008 ^d
NO	− 0.01942	N = − 0.04679 O = − 0.23325	− 0.15527	0.28252	− 0.18175	0.46	1.26	6.29	11 905 · 204	0.34 ^e

^a Mean charge of identical atoms.^b To get the relativistic electron densities multiply by 1.3.^c With respect to iron metal.^d G. E. Chappes, S. W. McCann, H. H. Wickman, and R. C. Sherwood, J. Chem. Phys. **60**, 990 (1974).^e C. E. Johnson, R. Rickards, and H. A. O. Hill, J. Chem. Phys. **50**, 2594 (1969).Table 3. Contributions to the electric quadrupole splittings in $[\text{Fe}(\text{dtc})_2\text{X}]$.

$[\text{Fe}(\text{dtc})_2\text{X}]$ with X	$C_{\text{Fe-L}}$ in Eq. (5)	Contributions to $1/2 eQ V_{zz}$ [mm s ^{−1}]					Total $1/2 eQ V_{zz}$ [mm s ^{−1}]	Calculated asymmetry parameter		Quadrupole splitting ΔE_Q [mm s ^{−1}]		Measured asymmetry parameter η
		overlap charge	ligand atoms	lattice	valence Fe 4p	shell Fe 3d		η_{3d}	η_{total}	calculated	measured	
NCS	0.5	− 0.002	0.003	− 0.001	− 0.05	2.09	2.04	0.55	0.22	2.11	2.65 ± 0.0 ^a 2.55 ± 0.01 ^b	—
Cl	0.5	1.06	− 0.87	0.018	0.06	2.40	2.66	0.38	0.21	2.71	2.70 ± 0.01 ^a	0.16 ± 0.01
Br	0.55	1.33	− 0.82	0.016	0.03	2.28	2.84	0.62	0.02	2.84	2.85 ± 0.01 ^a	—
I	0.58	1.34	− 0.78	0.011	0.0	1.80	2.37	0.95	0.33	2.90	2.89 ± 0.01 ^a	0.15 ± 0.03
NO	0.71	− 2.06	0.50	0.035	− 0.07	2.48	0.88	0.36	0.15	0.91	0.92 ^c	—

^a G. E. Chappes, S. W. McCann, H. H. Wickman, and R. C. Sherwood, J. Chem. Phys. **60**, 990 (1974).^b L. M. Epstein and D. K. Straub, Inorg. Chem. **8**, 560 (1969).^c B. Sarte, J. Stanford, W. J. La Price, D. L. Uhrich, R. E. Lockhart, E. Gelerinter, and N. Duffy, Inorg. Chem. **17**, 3361 (1978).

almost neutral or reach at a maximum $\sim |0.5|$ units of charge.

The iron atom has approximately an electronic configuration of $3d^{6.2}4s^{0.5}4p^{1.2}$ in contrast to that expected for an Fe^{3+} -ion $3d^54s^04p^0$. Care has to be taken in considering the iron 4s and 4p populations which may be unrealistic due to counterintuitive mixing [17]; but as the constant in (2) is relatively large, this effect is of minor importance. The charges on the ligand X also follow the order expected from their electronegativities, and NCS and NO have a charge distribution according to $N^{\delta-}C^{\delta+}S^{\delta-}$ and $N^{\delta+}O^{\delta-}$, respectively. An analysis based on the overlap charges between the atomic orbitals of the various atoms indicates that the Fe-S bond is predominantly of σ -type with

small π -contributions and that in the $\begin{array}{c} S \\ \diagup \quad \diagdown \\ C=N \end{array}$

fragment there is besides the σ -bonding a very strong π -delocalisation. A charge density analysis considering only the three unpaired electrons in the valence shell in the case of the $X=NCS$, Cl , Br , and I compounds (4A_2 ground state) and the one electron in the NO compound (2A_1 ground state) shows that the spin delocalisation from iron to the ligands results mostly from a π -delocalisation mechanism which is in excellent agreement with NMR results [2, 5].

The Isomer Shift

In a Mössbauer experiment the isomer shift δ , which is a measure of the electron density at the nucleus, $|\psi(0)|^2$ is given by [34]

$$\delta = \text{const} \cdot (\delta R/R) \{ |\psi(0)|_{\text{absorber}}^2 - |\psi(0)|_{\text{source}}^2 \}$$

where $|\psi(0)|_{\text{absorber}}^2$ is the charge density at the absorbing nucleus, $|\psi(0)|_{\text{source}}^2$ the charge density at the reference source nucleus and $\delta R/R$ the relative change of the nuclear radius in the excited and the ground state. The nuclear factor $\delta R/R$ for iron is negative, and therefore a positive isomer shift indicates a decrease of electron density at the absorbing nucleus. The electron densities $|\psi(0)|^2$ at the iron nucleus were calculated applying the formalism of Blomquist et al. [35] using the electronic configuration of the iron atom found from the MO calculations. The electron densities listed in Table 2, are almost constant within the series. The small variations in the calculated

electron densities indicate that the isomer shifts should follow the increasing positive order

$$\delta_{Cl} < \delta_{Br} < \delta_I < \delta_{NCS} < \delta_{NO}.$$

The ordering from Cl to NCS agrees well with that found from Mössbauer experiments [2]. From the calculated electron density, the nitrosyl compound is expected to have the highest positive isomer shift, which is contrary to the experimental observations. The formalism of Blomquist et al. considers only the potential distortion which arises from different electronic configurations but neglects the overlap distortion [34, 35, 36], which may be explicitly calculated by orthonormalising the inner iron core orbitals to all molecular orbitals. A mere comparison of differences in $|\psi(0)|^2$ in a series of complexes would imply the assumption that the overlap distortions and vibrational structures are the same in all cases and therefore may be neglected. The excellent agreement of the calculated ordering of electron densities in the series $X=Cl$, Br , I , NCS with the experimental isomer shifts implies that the overlap distortions and the vibrational structures along the series are similar. In the case of the nitrosyl complex the overlap distortions may play an important role in the calculations of $|\psi(0)|^2$. As the isomer shift contains also contributions from the second order Doppler shift, the poor correlation between δ and $|\psi(0)|^2$ in the case of the nitrosyl complex may also arise from differences in the vibrational structure in comparison with the other complexes.

Electric Field Gradient

a) At the Iron Nucleus

The population of the iron 3d-orbitals agrees well with that expected for a 4A_2 ground state: $(x^2 - y^2)^2(xz)^1(yz)^1(z^2)^1$; e.g. for $X=Cl$: $3d_{x^2-y^2} = 1.999$, $3d_{xz} = 1.061$, $3d_{yz} = 1.111$, $3d_{z^2} = 1.061$, and $3d_{xy} = 0.717$. Though the (xy) molecular orbital is not occupied in the ground state, the population analysis resulted in all cases in approximately 0.7 electrons in the iron $3d_{xy}$ atomic orbital, which is due to σ -bonding with the sulphur atoms. This population gives rise to a positive EFG and accounts for the large quadrupole splittings as the contributions of the other 3d orbitals nearly cancel each other.

Next the contribution to V_{zz} from the overlap charges is of importance. The overlap charges between ligand atoms are placed on the midpoint of the interconnecting line and the overlap charges between the iron atom and the ligand atom X, which are about 0.5 units of charge for the complexes with X = Cl, Br, I, NCS and approximately 0.9 for X = NO, are also situated at about one half of the iron-ligand bond length (see C_{FeL} in Table 3). The calculated value of V_{zz} is in all cases (except in the NO complex) not very sensitive to the empirical factor C_{FeL} in (5), which is $C_{\text{FeL}} \approx 0.5$, as the contributions to the EFG tensor from the overlap charges between iron and the four sulphur atoms nearly cancel the contribution from the overlap charge between iron and the axial ligand. In the nitrosyl complex the Fe-NO bond distance is 1.72 Å and thus a value of $C_{\text{FeL}} \approx 0.5$ would place the relatively large overlap charge very close to the iron nucleus and then the approximation $\gamma(r) = \gamma(\infty)$ is not valid. To compensate for the too large value of $1 - \gamma(r) = 10.1$, the overlap charges were placed more towards the ligand atoms L using the larger value of $C_{\text{FeL}} = 0.71$. Then V_{zz} is positive and the measured quadrupole splitting can be achieved. If a value of $C_{\text{FeL}} = 0.5$ is assumed, the calculated V_{zz} becomes very large and negative. To confirm the validity of the used approximation ($C_{\text{FeL}} = 0.71$) V_{zz} was calculated by numerical integration [10] with an explicit functional form of the Sternheimer shielding factor $\gamma(r)$ in (4). The numerical integration was carried out by considering about $2.5 \cdot 10^5$ points of electron density in space, using (4) with a value of $\gamma(r) = 0.32$ up to 0.7 Å and then decreasing it linearly to the final value of -9.1 at $r = 1.0$ Å. The sign of V_{zz} was found to be positive but the absolute value of the calculated quadrupole splitting was about twice the measured value. This may be due to the simple functional form used for $\gamma(r)$ and to the incorrect radial behaviour of the iron 3d double zeta function near the iron nucleus. However, the positive sign of V_{zz} calculated by numerical integration justifies the adopted value of $C_{\text{FeL}} = 0.71$ in the nitrosyl complex.

The contribution to V_{zz} in the NO complex from the iron 3d shells $\frac{1}{2}eQV_{zz} = 2.48 \text{ mm s}^{-1}$ * is very similar to those found in the other compounds, but

* For ^{57}Fe (14.4 keV); $1 \text{ mms}^{-1} = 11.6248 \text{ MHz}$; for ^{129}I (27.8 keV); $1 \text{ mms}^{-1} = 22.398 \text{ MHz}$.

the relatively large overlap charge contributes with opposite sign and diminishes V_{zz} . This accounts for the small observed quadrupole splitting of the NO complex.

Contrary to an earlier crystal field calculation [7] where the main contribution to the EFG was assumed to arise from the lattice, the present calculation shows that the lattice contributions of the 2000 next nearest neighbours are very small.

The asymmetry parameter η calculated from the 3d contribution varies from 0.4 to 0.9. The contributions from the 4p electrons, lattice and ligand increase V_{yy} and decrease V_{xx} , result finally in much smaller values of $0.15 \leq \eta \leq 0.33$ which are in reasonably good agreement with the experimental results.

b) At the Iodine Nucleus

Using the MO results, the EFG at the iodine nucleus was calculated using the same formalism as in the case of iron. The main contribution giving rise to a positive V_{zz} comes from a hole of 0.48883 electrons in the iodine 5p_z orbital ($5p_x = 1.53117$). The coupling constant eQV_{zz}^{val} , using (5) with $R_{5p} = 0.0$, $\langle r^{-3} \rangle_{5p} = 14.87$ [37] and $Q = -0.55 \text{ b}$ [38], is $eQV_{zz} = -30.1407 \text{ mm s}^{-1}$. The ligand and lattice contributions calculated using (4) as a point charge approximation taking into account about 2000 nearest neighbours with $\gamma(\infty) = -13.3$ [39] gave $eQV_{zz}^{\text{lig+lattice}} = -0.2198 \text{ mm s}^{-1}$. The overlap charge of $q_{\text{Fe-I}} = -0.69657$ between iodine and iron is situated more towards the iodine atom, and by using a value of $C_{\text{I-Fe}} = -0.336$ in (9) and the actual value of the Sternheimer shielding factor for iodine in the overlap region [39] $\gamma = -16.1$ ($r = 0.87 \text{ Å}$), the measured quadrupole coupling constant [40] $eQV_{zz}^{\text{exp}} = -14.9 \text{ mm s}^{-1}$ is best obtained from all contributions. The overlap charge contribution $eQV_{zz}^{\text{overlap}}$ was calculated to be 15.48 mm s^{-1} .

Acknowledgements

One of the authors (P.G.) gratefully acknowledges the Alexander von Humboldt Foundation, Western Germany for the award of a fellowship (July 1977 to August 1979) and (K.H.) is grateful to the Deutsche Forschungsgemeinschaft for financing a part of this work. The authors also thank Prof. H. H. Wickman for supplying Dr. W. Sly's unpublished structural data on $[\text{Fe}(\text{dtc})_2\text{NCS}]$.

- [1] R. L. Martin and A. H. White, *Inorg. Chem.* **6**, 712 (1967).
- [2] G. E. Chapps, W. W. McCann, H. H. Wickman, and R. C. Sherwood, *J. Chem. Phys.* **60**, 990 (1974).
- [3] P. Ganguli, V. R. Marathe, and S. Mitra, *Inorg. Chem.* **14**, 970 (1975).
- [4] N. Arai, M. Sorai, H. Suga, and S. Seki, *J. Phys. Chem. Solids* **38**, 1341 (1977).
- [5] M. M. Dhingra, P. Ganguli, V. R. Marathe, S. Mitra, and R. L. Martin, *J. Mag. Res.* **20**, 133 (1975).
- [6] J. H. Enemark and R. D. Feltham, *Coord. Chem. Rev.* **13**, 339 (1974).
- [7] R. L. Ake and G. M. H. Loew, *J. Chem. Phys.* **52**, 1098 (1970).
- [8] J. L. K. F. DeVries, C. P. Keijzers, and E. DeBoer, *Inorg. Chem.* **11**, 1343 (1972).
- [9] J. L. K. F. DeVries, Ph. D. Thesis, Nijmegen University March (1972).
- [10] R. Hoffman, *J. Chem. Phys.* **39**, 1397 (1963).
- [11] First results are published in *J. de Physique* "International Conference on Mössbauer Spectroscopy", Portoroz, Yugoslavia, 10.—14.09.1979.
- [12] All the computer programs used in the present calculations were written by K. M. Hasselbach.
- [13] A. M. Schaffer, M. Gouterman, and E. R. Davidson, *Theoret. Chim. Acta* **30**, 9 (1973).
- [14] M. Zerner, M. Gouterman, and H. Kobayaski, *Theor. Chim. Acta* **6**, 363 (1966).
- [15] A. Trautwein, R. Zimmermann, and F. E. Harris, *Theoret. Chim. Acta* **37**, 89 (1975).
- [16] K. M. Hasselbach, *J. Physique* **37**, C6—457 (1976).
- [17] J. H. Ammeter, H.-B. Burgi, J. C. Thibault, and R. Hoffmann, *J. Amer. Chem. Soc.* **100**, 3686 (1978).
- [18] J. C. Slater, *Phys. Rev.* **36**, 57 (1930).
- [19] R. Manne, K. Wittel, and B. S. Mohanty, *Mol. Phys.* **29**, 485 (1975).
- [20] J. W. Richardson, W. C. Nieuwport, R. R. Powell, and W. F. Edgell, *J. Chem. Phys.* **36**, 1057 (1962).
- [21] G. R. Davies, J. A. J. Jarvis, B. T. Kilbourn, R. H. B. Mais, and P. G. Owston, *J. Chem. Soc. (A)* 1275 (1970).
- [22] B. F. Hoskins and A. H. White, *J. Chem. Soc. (A)* 1668 (1970).
- [23] P. C. Healy, A. H. White, and B. F. Hoskins, *J. Chem. Soc. Dalton Trans.* **1972**, 1369.
- [24] Structural data on $[\text{Fe}(\text{dte})_2\text{NCS}]$, W. G. Sly (private communication).
- [25] G. E. Chapps, S. W. McCann, and H. H. Wickman, *J. Chem. Phys.* **60**, 990 (1974).
- [26] L. M. Epstein and D. K. Straub, *Inorg. Chem.* **8**, 560 (1969).
- [27] B. Bleaney, *Hyperfine Structure and Electron Paramagnetic Resonance*; A. J. Freeman and B. R. Frankel (ed.), *Hyperfine Interaction*, Academic Press, New York 1967.
- [28] H. M. Foley, R. M. Sternheimer, and D. Tycko, *Phys. Rev.* **93**, 734 (1954).
- [29] P. Ganguli, Ph. D. thesis "Magnetic and Spectroscopic Studies on Ferric Dithiocarbamates" pp. 181, University Bombay, India, October 1976.
- [30] H. B. Gray, I. Bernal, and E. Billig, *J. Amer. Chem. Soc.* **84**, 3404 (1962).
- [31] A. Goodman, J. B. Raynor, and M. C. R. Symons, *J. Chem. Soc. (A)* **1969**, 2572.
- [32] M. S. Hunt and R. D. Feltham (unpublished results).
- [33] S. A. Best, P. Brant, R. D. Feltham, T. B. Rauchfuss, D. M. Roundhill, and R. A. Walton, *Inorg. Chem.* **16**, 1976 (1977).
- [34] P. Gülich, R. Link, and A. Trautwein, *Mössbauer Spectroscopy and Transition Metal Chemistry*, Springer-Verlag, Berlin 1978.
- [35] J. Blomquist, B. Roos, and M. Sundbom, *J. Chem. Phys.* **55**, 141 (1971).
- [36] J. C. Chang, T. P. Das, and D. J. Kenberry, *Theoret. Chim. Acta* **35**, 361 (1974).
- [37] S. Fraga, J. Karwowski, and K. M. S. Saxena, *Handbook of Atomic Data*, Elsevier Scientific Publishing Company, New York 1967.
- [38] R. Livingston and H. Zeldes, *Phys. Rev.* **90**, 609 (1953).
- [39] S. Lauer, V. R. Marathe, and A. Trautwein, *Phys. Rev. A*, **19**, 1852 (1979).
- [40] D. Petridis, A. Somopoulos, A. Kostikas, and M. Pasternak, *J. Chem. Phys.* **65**, 3139 (1976).